Nucleation of the electroactive γ-phase and enhancement of the optical transparency in low filler content poly(vinylidene)/clay nanocomposites

A.C. Lopes[1, 2], C.M. Costa[1], C. J. Tavares[1], I. C. Neves[2], S. Lanceros-Mendez[1, *]

[1]*Center/Department of Physics, University of Minho, Campus de Gualtar, 4710-057 Braga, Portugal*

[2]*Department of Chemistry, University of Minho, Campus de Gualtar, 4710-057 Braga, Portugal*

Abstract

Poly(vinylidene fluoride), PVDF, based nanocomposites with different clays structures have been processed by solvent casting and melt crystallisation. Depending on the melting temperature of the polymer, the nanocomposite recrystalises in the electroactive γ or non electroactive α-phase of the polymer. This fact is related to the thermal behaviour of the clay. For montmorillonite clay, the full crystallisation of the electroactive γ-phase occurs for clay contents lower than 0.5 wt%, allowing the nanocomposites to maintain the mechanical properties of the polymer matrix. The electroactivity of the material has been proven by measuring the piezoelectric d_{33} response of the material. The obtained value of d_{33} is -7 pC/N, lower than in β-PVDF obtained by mechanical stretching, but still among the largest coefficients obtained for polymers. Further, the optical transmittance in the visible range is strongly enhanced with respect to the transmittance of the pure polymer. Finally, it is demonstrated that the nucleation of the γ-phase can be also obtained in other clays, such as in kaolinite and laponite.

PACS: 77.84.-s; 85.50.-n; 77.65.-j

* Electronic mail: lanceros@fisica.uminho.pt

Keywords: electroactive polymers; sensor and actuators; piezoelectric; functional graded materials

Introduction

The mixing of polymers and clays has been widely investigated in recent years mainly due the mechanical reinforcement effect of the latter. The main goal has been to replace traditional fibre reinforced composites due to improved strength and stiffness stability, thermal and barrier properties and flame retardant behaviour of the clay nanocomposites.[1,2,3] One interesting polymer for nanocomposites production is poly(vinylidene fluoride), PVDF, due to its remarkable electroative properties and therefore its suitability for sensor and actuator applications. Furthermore, PVDF films present high flexibility, high mechanical resistance, dimensional stability, lightness, moldability, low cost production and low mechanical and acoustic impedance.[4] Depending on the processing conditions PVDF, with a chemical formula $(CH2\text{-}CF2)_n$, can crystallise in at least four different phases: α, β, γ and δ.[5,6] The α-phase, that has an alternating *s-trans* and *s-gauche* C-C bonds, is the most stable when the material is cooled from the melt and therefore the most commonly obtained.[5] The β-phase, with all C-C bonds in the s-*trans* conformation (TTTT), is the one that presents the best electroactive piezoelectric and pyroelectric properties and is commonly obtained by mechanical stretching of the α-phase[7] or by the addition of selected nanoparticles.[8,9] The γ-phase is, as the β-phase, electrically active. However, due the presence of a g-*gauche* bond every fourth repeat units of C-C band ($T_3GT_3\bar{G}$), this effect if weaker when compared with β-phase. γ-phase can be obtained by crystallization from the melt or solution casting at temperatures near the melt temperature of the α-phase. The α→γ solid state phase transformation also can occur by annealing at temperatures close to melt temperature.[10]

In the last years, the literature reports some studies where organically modified clays show the ability to induce, by melt intercalation or solution casting, the crystallization of the electroactive β-phase of PVDF[11-14] and, in a few studies, the induction of a crystalline γ-phase.[14,15]

The distribution, intercalation and exfoliation of organically modified silicates prepared from Cloisite and Montmorillonite clays has been investigated and it is concluded that the trend of PVDF to crystallize in the β-phase is higher in organically modified clays when compared with unmodified clays.[11] In all cases, the full β-phase crystallization is obtained by inclusion of an amount of clay higher than 1.5 wt%.[16]. The full β-phase crystallization of PVDF has also been achieved for lower clay contents, of the order of 0.025 %, by an improved method; however, this method implies a very high consumption of material.[13] In general, the toughness of nanocomposites, the melting and crystallization temperature and also the crystallization rate increases with the introduction of nanoparticles and, conversely, the crystallinity of the nanocomposites decreases.[16-18]

On the other hand, a few number of more recent studies indicate that the γ-phase of PVDF is nucleated in the presence of the organoclays. It was demonstrated that when the composite samples are subjected to a slow cooling from the melt, the presence of the organoclays induce the crystallization of a mixture of γ-phase and α-phase, the γ-phase being predominant for organoclay concentrations above 1.5 wt%[15]. On the other hand, when the sample is subjected to a melt-quenched-annealing process, the nanocomposites crystallize in a mixture of β- and γ-crystals[15]. Finally, a recent study concluded that though the melt-crystallization at hight supercooling the γ-phase is also obtained for an organoclay content up to 0.1%, in contrast to cold-crystallized samples, where organoclays addition results in β-phase PVDF[14].

Some of the results presented in the above mentioned articles are contradictory, which result from the confusion generated on the identification of the γ- and β-phase. Due to the s-*trans* conformation (TTTT) of the β-phase of PVDF and the ($T_3GT_3\bar{G}$) conformation of the γ-phase of the polymer, their characteristic FTIR bands and X-ray diffraction bands typically used for the identification of the phases either coincide or are very close to each other, making difficult to distinguish it. Based on literature results, the analysis of Table 1 allows to precisely identifying the FTIR absorption bands of the crystalline phases of PVDF.

Table 1. FTIR absorption bands characteristics of the α-, β- and γ-phases of PVDF[19-22]

α-phase (cm^{-1})	**β-phase** (cm^{-1})	**γ-phase** (cm^{-1})
408	445	431
532	467	440
614	510	512
764	840	776
796	884	812
855	1175	833, 838
976	1275	883
1149		
1210		1234
1383		1117

From Table 1 it is important to notice that most of the bands typically used for the identification of the electroactive β- and γ-phases of the polymer, in particular those at 510, 512, 833, 838, 840, 883 and 884 cm^{-1} (shadow in Table 1) are actually superposition of β- and γ-phase absorption bands, when both phases exist. On the other hand, just the peaks at 445 and 467 cm^{-1} are characteristic absorption bands of the β-

phase without superposition with other absorptions and just the absorption bands at 431, 812 and 1234 cm^{-1} are characteristic of the γ-phase without superposition with absorptions from other phases[19-22].

Further, in the previous articles reporting on the nucleation of the electroactive phase of the polymer by clays, the piezoelectric response and optical properties of the material has never been discussed, which are the key issues for the use of the material in sensor and actuator applications.

In the present work, the main problems that exist in the processing of electroactive PVDF through the nucleation with clays are addressed. It is shown that it is possible to prepare PVDF/clay nanocomposite in the γ-phase with low clay contents, without any organic treatment and with a low consumption of material. Moreover, the material presents increased transmittance in the visible range, making it appropriate for optical applications. It is also shown that the material can be poled and the d_{33} piezoelectric coefficient has been measured as a function of the clay and the γ-phase contents. Finally, it is shown that different clays can be used in order to achieve the electroactive polymer phase.

Experimental

PVDF/clay nanocomposites with an average thickness of 50 μm were prepared by spreading a solution of 1.0 g of PVDF powder (Solef 1010) with a suspension of montmorillonite K10 (Aldrich) in 4 mL of N,N-dimethyl formamide (DMF) in a glass slide. Previously, the suspension of montmorillonite and DMF was homogenized by placing it in an ultrasound bath for 4h before the polymer was added and dissolved with

a magnetic stirrer. After this process the nanocomposite is typically melted at 210ºC and recrystallised to room temperature.[23] Since the clay can suffer structural modifications at this temperatures[24-25], six films with a clay concentration of 0.50 wt% were prepared at temperatures between 170 ºC and 220 ºC in order to study the effect of the polymer melting temperature during nanocomposite preparation. The effect of clay concentration on the electroactive phase content was further studied in films with 0.10, 0.25 and 0.50 wt% of montmorillonite. Finally, the effect of different clay structures was studied by incorporating an amount of 0.50 % of kaolinite (from North of Portugal) and laponite (Laport Industries Ltd) into the polymer matrix by the same procedure explained above.

Scanning Electron Microscopy (SEM) was performed using a FEI Nova 200 NanoSEM with an acceleration voltage of 15 kV in order to evaluate the morphology and microestructure of the clay and the nanocomposite.

The crystalline phase of PVDF on the nanocomposites was determined by Fourier Transformed Infrared Spectroscopy (FTIR) in the ATR mode (Spectrum 100, Attenuated Total Reflectance mode) in the range between 650 and 4000 cm^{-1}, on 32 scans.

X-ray diffraction (XRD) measurements were carried out in a X'Pert Pro-MPD advanced diffractometer equipped with Cu K_α radiation operated at 50 kV and 40 mA in order to study the polymer phase and clay behaviour.

Differential scanning calorimetry (DSC) was performed in a Mettler Toledo DSC 823 apparatus under a nitrogen atmosphere at a heating rate of 10 ± 0.2ºC.min^{-1} in order to evaluate the crystalline fraction of the polymer and the influence of the clay on the melting behaviour.

In order evaluate the piezoelectric response of the samples, films were first subjected to a *Corona* discharge under previously optimized conditions of 70 ºC of temperature inside a home-made chamber under an electric field of 30 kV and a constant current of 15 µA during 75 minutes. Still under the application of the field, the films were cooled down to 30ºC. The piezoelectric d_{33} response was measured with a Wide Range d_{33}-meter (Model 8000, APC Int Ltd).

The complex dielectric constant as a function of frequency was measured between 100 Hz and 1 MHz with an automatic Quadtech 1929 Precision LCR meter, after thermal deposition of gold electrodes on the sample.

Measurements of optical transmittance were performed with an optical spectrophotometer Shimatzu UV-3101PC in the range of 400 to 700 nm.

Dynamic mechanical analysis was performed with a DMA 8000 Perkin-Elmer set-up in the nanocomposites with different clay types and a clay concentration of 0.5 %. The measurements were performed at room temperature with a frequency scan from 0.01 to 10 Hz.

Results and Discussion

a) Effect of the melting temperature

PVDF films are usually prepared by solution cast and melting at a range of temperatures higher than 200ºC[17], which corresponds to the temperature of clays interlayer water elimination and therefore a temperature range in which structural modifications can occur.[24-25] Due this fact, it becomes important to study the influence of the melting

temperature in the final properties of the nanocomposites, as the clay/polymer interfacial interaction will be modified during the crystallisation of the polymer matrix. In order to study this effect, nanocomposites of PVDF with 0.5 %wt of montmorillonite were melted at different temperatures and cooled to room temperature. Fig.1 shows FTIR-ATR patterns of the samples prepared after melting at different temperatures.

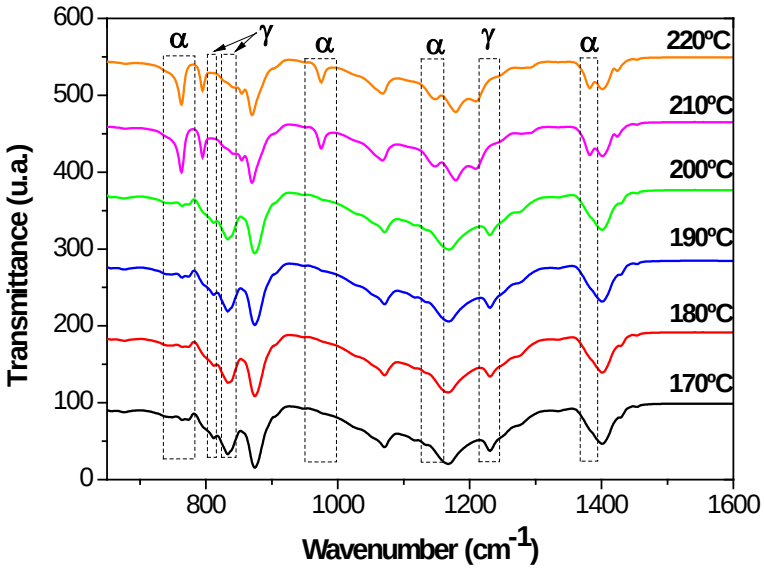

Figure 1. FTIR-ATR spectra of PVDF/clay nanocomposite melted at different temperatures

It can be concluded from Figure 1 that the melting temperature affects the crystalline polymer phase present in the nanocomposite, as identified by specific clear differences in the FTIR spectra. For the calculation of the relative amount of each polymorph present in the polymer, some bands between 700 and 1500 cm^{-1} of the FTIR spectra have been identified to correspond to the α-, β and γ-phases of the polymer (Table 1)[26] and can be used for this purpose.

As previously mentioned, the proximity or even the superposition of FTIR absorption bands of the β- and γ-phase of PVDF led to a large number of contradictions in the phase identification of nanocomposites. However, the analysis of the FTIR spectra in parallel with Table 1 and with the support of recent studies [14,15] allows to conclude that nanocomposites of PVDF with clays melted at a temperature not exceeding 200ºC fully crystallize in the γ-phase. In particular, Figure 1 shows a strong decrease of the 764, 976, 1149 and 1383 cm^{-1} bands, characteristics from the α-phase with respect to the nanocomposites prepared after melting at higher temperatures. On the other hand, the peaks at 812, 833, 838 and 1234 cm^{-1}, characteristics of the γ-phase, suffer a strong increase. No representative amount of β-PVDF is identified in the samples as no characteristic peaks identified just with this phase suffer any modification with the processing temperature (Table 1), as it is proved to occur when this phase is nucleated in other clay nanocomposites[14, 15].

The relative amount γ-phase (*F(γ)*) present in the samples and shown in Table 2 was calculated applying a previously developed method (equation 1) for the quantification of the polymer phase content[7,27,28] , assuming that the crystalline phase content of the polymer is either in the α or γ-phase[20], with no or small traces of β-phase:

$$F(\gamma) = \frac{X_\gamma}{X_\alpha + X_\gamma} = \frac{A_\gamma}{(K_\gamma / K_\alpha)A_\alpha + A_\gamma} \quad (1)$$

Here, A_α and A_γ represent the absorbencies at 766 and 833 cm^{-1}, which correspond to the *α*- and the *γ*-phase material; K_α and K_γ are the absorption coefficients at the respective wave numbers and X_α and X_γ the degree of crystallinity of each phase. The value of K_α is 0.365 and the value of K_γ is 0.150 μm^{-1}.[20]

When the melting of the nanocomposite occurs at temperatures above 210ºC, the polymer recrystallizes in the α-phase and this tendency increases for higher temperatures. On the other hand, when the material is melted at temperatures below 200ºC, it tends to crystallize in the γ-phase (Table 2). It should be stressed that this fact does not occur in the absence of the clays, when the polymer always crystallises in the α-phase independently of the previous melting temperature of the material.

Table 2. γ-phase content, calculated by equation 1, for PVDF/montmorillonite nanocomposites obtained by recristallization after melting at different temperatures.

Temperature (ºC)	Percentage of γ-phase (%)
170	97
180	98
190	96
200	95
210	0
220	0

The nucleation of the electroactive γ-phase is due to an interaction between the negatively charged delaminated clays and the dipolar moments of the PVDF. This ion-dipole interaction tends to order the PVDF monomers in a preferentially *trans* conformation inducing therefore the crystallization of the γ- or β-phases.[15] The stabilization of either γ or β-phase is not understood and depends on factors such as cooling rate and surface modification of the clays[14, 15].

On the other hand, by increasing meting temperature, the reduction of the interlayer spacing of the clays at temperatures above 200 ºC due the elimination of interlayer

water[25] prevents the exfoliation of montmorillonite which in turn reduces the contact area between the negatively charged delaminated clays and the dipolar moments of PVDF, preventing its crystallization of the electroactive phases. The interlayer water elimination and the collapse of the interlayer distance is confirmed by the disappearance of the $d_{(001)}$ diffraction peak[29], attributed to the interlayer distance, at $2\theta \approx 9^{o}$, in the XRD patterns for samples prepared at temperatures above the 200ºC (Fig. 2 a) and b), inset).

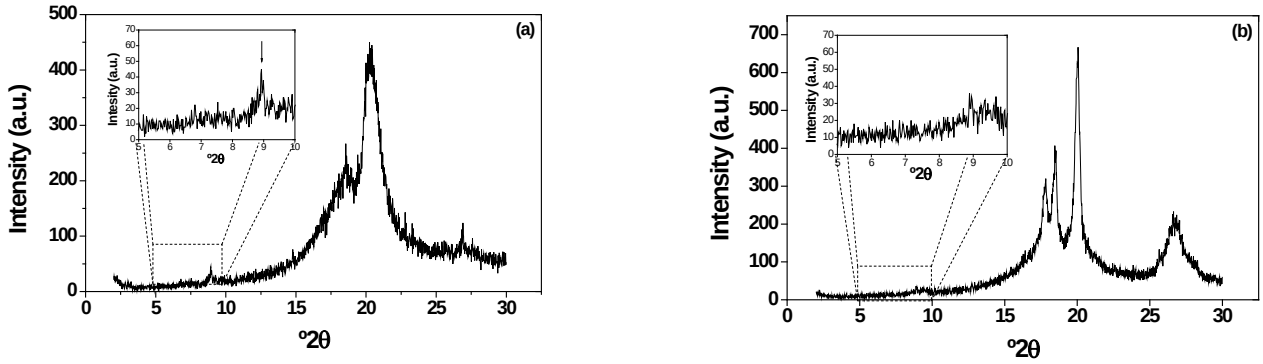

Figure 2. XRD patterns for PVDF/clay nanocomposite melted at 200 ºC (a) and 210 ºC (b), respectively.

The XRD patterns also confirm that when the sample is melted at 210ºC it crystallizes in the α-phase of PVDF, with characteristic peaks at 17.7, 18.4 and 19.9º and that when the sample is melted at 200ºC, the XRD patterns show the peaks at 18.5, 19.2, 20.1, 20.3 and 26.8, characteristic of the γ-phase (Figure 2).

With respect to the morphology of the composites, SEM images (Fig. 3) show a uniform distribution of the clay within the polymer matrix and a non-porous, compact microstructure of the polymer matrix, independently of the melting temperature.

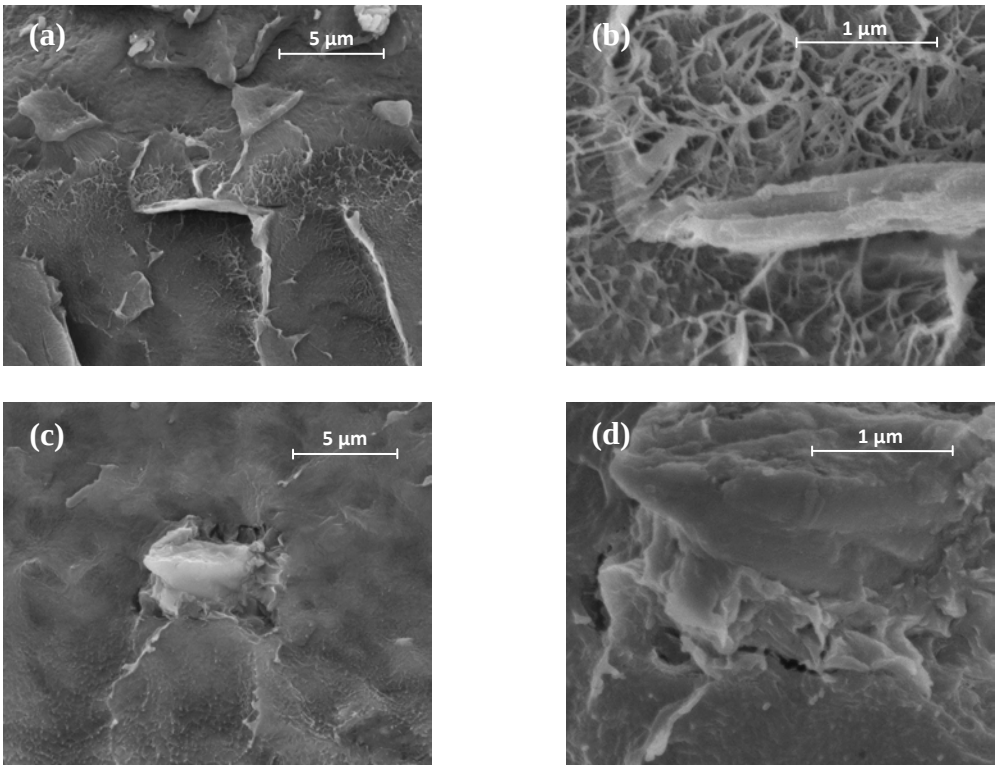

Figure 3. Scanning electron microscopy (SEM) micrographs of the nanocomposites with 0.5% of montmorillonite melted at 170ºC (a), (b) and 220ºC (c), (d).

On the other hand, as observed in Fig. 3, the montmorillonite microstructure changes for the different nanocomposite prepared after melting at different temperatures. For the samples prepared at lower temperatures (Fig. 3, a and b), platelets of some nanometric layers are well separated one another and dispersed in different directions along the continuous polymer matrix. In this situation, there is a larger interaction area between these clay platelets of montmorillonite and the polymer (Fig. 3(b)), the polymer microstructure growing from the clay layers. On the other hand, when the polymer is melted at temperatures above 200ºC, the clays create larger micrometer size clusters due to the interlayer structural variations. This fact reduces the interaction area between the clays and the polymer matrix and do not promote the crystallization of the electroactive phase.

The composites in the α- and γ-phases show also different optical transmittance to the visible light. Measurements of optical transmittance are presented in Fig. 4, demonstrating that for melting temperatures equal or less than 200 ºC the transmittance in the visible region of the nanocomposite is much higher than for the melting temperatures above it. This fact is attributed to the variations of the clay microstructure and its dispersion in the polymer matrix, as well as its influence, as it will be shown later, on the degree of crystallinity of the polymer. As observed in Figure 3, for processing temperatures below 200 ºC the dispersion of the clays is better achieved, as well as the wetting by the polymer. Further, the clay is dispersed in the form of small platelets of some clay nanometric layers. These factors imply a better optical transmittance than the larger clay grains not so well dispersed and with worst interaction with the polymer matrix obtained for the samples melted at higher temperatures, that create defective microstructure e.g. voids and cracks (Fig. 3 c, d).

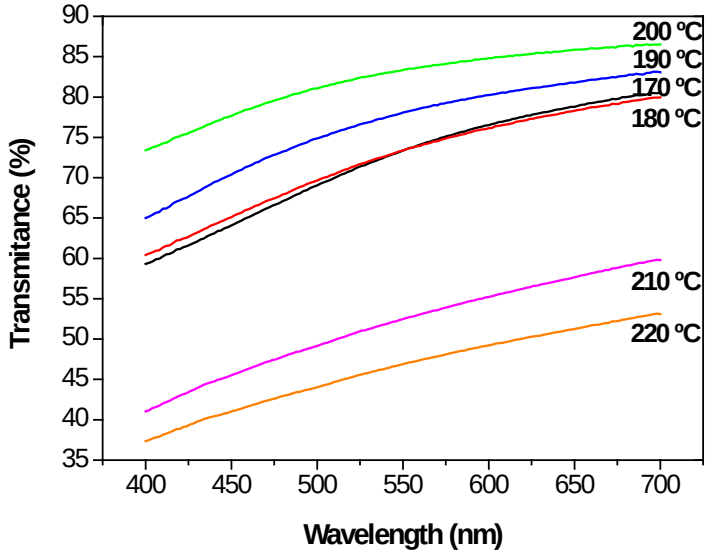

Figure 4. Optical transmittance in the visible range of PVDF/ montmorillonite nanocomposites after processing at different melting temperatures

Fig. 4 also shows that the transmittance of the films is higher as the melting temperature approaches 200ºC. Thus, it seems to be an ideal melting temperature for obtaining highly transparent piezoelectric nanocomposites.

b) Functionally graded electroactive composites

The relationship between the processing temperature and the polymer phase after recrystalisation allows the production of samples with different electroactive phase content and transmittance along the films, with potential application as functionally graded materials in electrical, optical and electrooptical areas.[30,31] This effect can be achieved by exposing different parts of the film to different temperatures. In this way, a film of 14 cm was exposed to a temperature gradient from ~210 to 180 ºC along its length and the optical transmittance and phase content were determined at different points 2 cm apart along the film (the points were numbered 1 to 6, from the higher to the lower temperature side). The results are presented in Fig. 5.

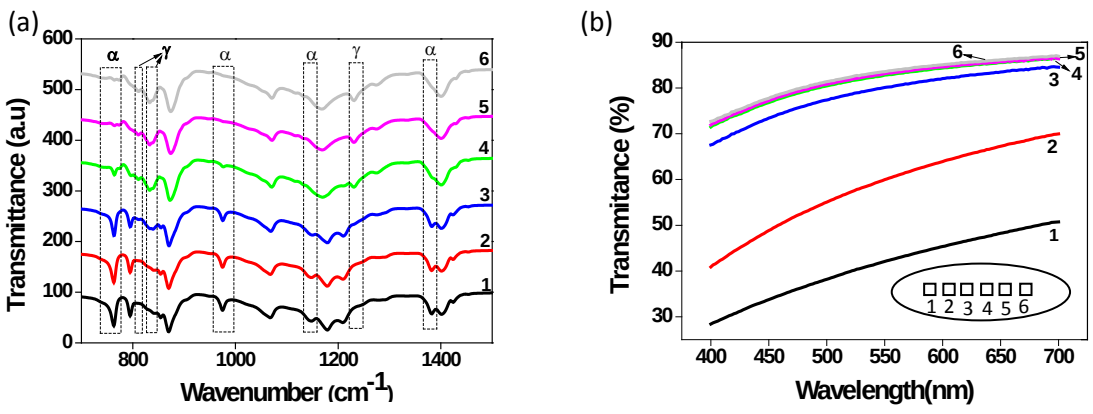

Figure 5. FTIR-ATR spectra of functionally graded film of PVDF/montmorillonite (a) and the corresponding optical transmittance spectra in the visible region (b)

Fig. 5 (a) shows the gradual decrease of the peak at 764, 976, 1149 and 1383 cm^{-1} indicative of the presence of the α-phase and the increase of the peaks at 812, 833, 838 and 1234 cm^{-1} related to the γ-phase. The quantification of the electroactive phase content in each of the sites of the sample by Equation (1) is presented in Table 3.

Table 3. γ-phase content, calculated by equation 1, for the PVDF/montmorillonite nanocomposite film melted in a temperature gradient.

Position	Percentage of γ-phase (%)
1	0
2	0
3	37
4	81
5	95
6	97

It is demonstrated in this way that the electroactive γ-phase content ranges from 0 to 97% and that it is also accompanied by a gradual increase on the transmittance of the film (Fig 5 (b)).

c) Effect of the clay content

The effect of relative amount of clay in the electroactive phase content of the nanocomposite was evaluated by preparing samples with 0.10, 0.25 and 0.50 %wt of montmorillonite within the polymer matrix and by melting the nanocomposites at 200ºC. FTIR results reveal that the γ-phase content is also dependent on the clay content (Fig. 6).

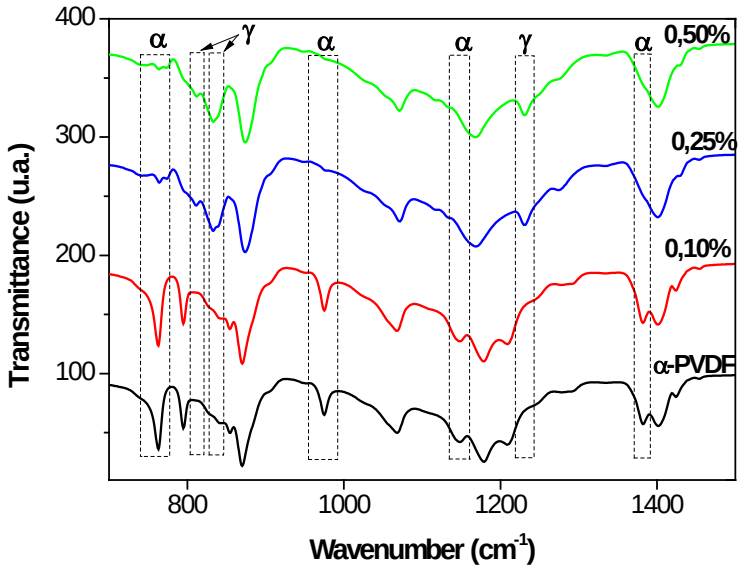

Figure 6. FTIR-ATR spectra of PVDF and PVDF with different percentage of montmorillonite prepared after melting at 200 ºC.

The γ-phase content, presented in table 4, was calculated using Equation 1 and the 764 and 833 cm^{-1} absorption bands.

Table 4. γ-phase content, degree of crystallinity and d_{33} for nanocomposites with different amounts of montmorillonite

Montmorillonite (wt %)	γ-phase (%)	Crystallinity (%)	d_{33} (pC/N)	ε' (f = 1kHz)	tg δ (f = 1kHz)
0.00	0	47	0	7.3	0.0389
0.10	0	40	0	8.5	0.0200
0.25	84	49	-7	10.2	0.0274
0.50	91	50	-6	9.7	0.0391

The introduction of 0.10 wt% of montmorillonite does not affect the crystalline phase of the polymer, crystallizing mainly in the nonelectroactive α-phase. However, when 0.25 wt% of montmorillonite is introduced there is a decrease of the 764, 976, 1149 and 1383 cm^{-1} peaks, characteristics of the α-phase and a corresponding appearance of the 812, 833-838 and 1234 cm^{-1} peaks, assigned to the γ-phase.[7] The increase of montmorillonite concentration induces even further the nucleation of the γ-phase. For a percentage of 0.50 wt%, the α-phase completely disappears and the γ-phase is further enhanced, at a maximum value of ~ 90%. Table 4 also shows the degree of crystallinity of the polymer composites as measured by DSC (Fig. 7) and calculated by Equation (2):

$$\Delta X_c = \frac{\Delta H_f}{\Delta H_{100}} \quad (2)$$

where ΔH_f represents the melting enthalpy of the composite and ΔH_{100} (taken as 104,6 J/g) [20] is the melting enthalpy for a 100% crystalline sample of pure PVDF.

It is observed that the degree of crystallinity is affected by the amount of clay present in the composite. The composite shows a decrease of the degree of crystallinity when the clay, for small clay concentrations, acts as a defect in the polymer structure, with no capability of nucleation of the electroactive phase. Further, by increasing clay content the clay seeds act as nucleating agents of the γ-phase and the degree of crystallinity increases.

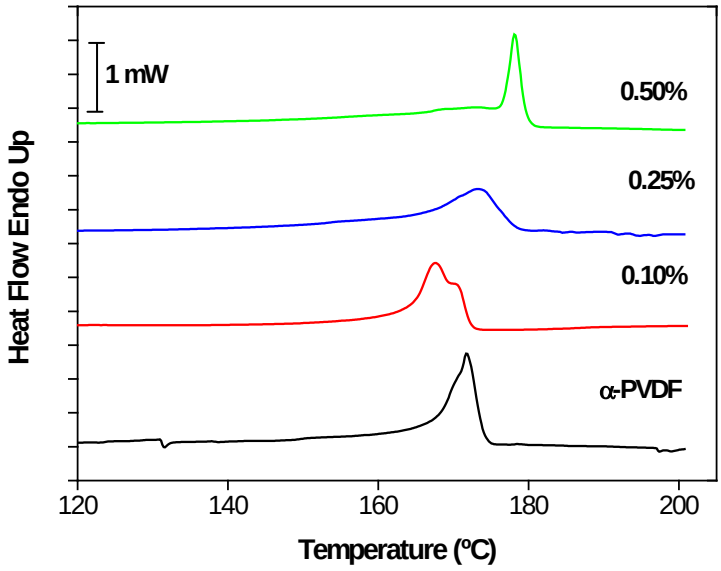

Figure 7. DSC thermograms for α-PVDF and PVDF with different percentage of montmorillonite.

The aforementioned behaviour is supported by the shape of the DSC scans (Fig. 7) obtained for the first heating runs obtained for nanocomposites with different amount of montmorillonite. The samples with 0.10 %wt of clay maintain the melting peak at the same temperature as the α-phase of PVDF, with a shoulder associated to the presence of defects in the films due to the introduction of clays. As the amount of clay is increased, the melting peak is shifted to higher temperatures. When the clay reaches a

0.50%wt concentration, the peak is at 178ºC what corresponds to the melting of the γ-phase crystals.[10]

Finally, the crystallization of the samples in the γ-phase is further demonstrated by their piezoelectric d_{33} response (Table 3). It is noteworthy to mention that the piezoelectric coefficients, despite being lower than for the β-phase of the polymer, they are still among the largest obtained for polymers, are in the range suitable for application and are obtained avoiding the stretching process necessary to prepare β-PVDF, which hinders many applications involving microfabrications techniques.[32] The lower piezoelectric response of γ-PVDF with respect to β-PVDF mainly relies in the different chain conformations, with more dipolar moments for unit cell contributing to the electroactive response in the all-trans chain conformation of β-PVDF. Finally, there is also a contribution of the microstructure to the reduction of the electroactive response: in the present case, films crystallize in a spherulitic microstructure with random orientation of the polymer chains, conversely to the stretched films that show preferential chain and crystallite orientation.[33] Finally, the values for the real and imaginary parts of the dielectric constant are similar to the ones obtained for β-PVDF[5] (Table 3).

d) Effect of the different clays

In order to further evaluate the origin of the crystallization of the γ-phase of PVDF by clays, nanocomposites of clays with different structures were prepared for a given clay content: montmorillonite, laponite and kaolinite. Montmorillonite is an expanding clay with a structure type of 2:1. When exfoliated, it creates plates with a thickness of 1 nm

and a diameter ranging from 50 to 500 nm. Laponite has the same 2:1 clay structure type of montmorillonite, but it shows mesoporosity resulting from interparticle aggregates and can create platelets of 1nm of thickness but with a smaller diameter than monmorillonite (~30 nm).[34] Kaolinite present a 1:1 clay structure type, it has a basal spacing fixed at 0.72 nm and, unlike the aforementioned clays, is unable to absorb water into the interlayer position. All the samples were prepared by solvent cast at a concentration of 0.5 %wt and melted at 200ºC. The results obtained by FTIR are presented in Fig. 8.

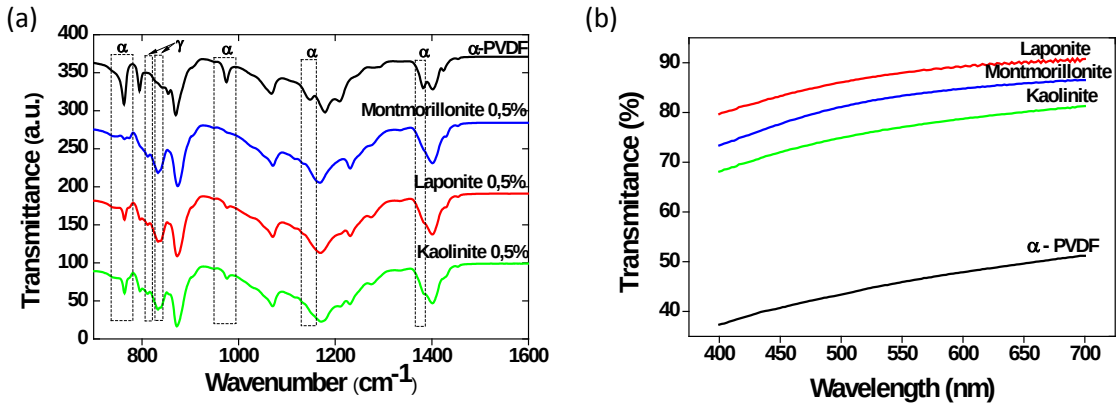

Figure 8. a) FTIR-ATR spectra of nanocomposites of PVDF with 0.5%wt of montmorillonite, laponite and kaolinite clays and b) the corresponding optical transmittance spectra in the visible region.

Fig. 8 (a) shows that the γ-phase content is more pronounced in montmorillonite samples, followed by laponite and finally by kaolinite. The piezoelectric γ-phase content, as calculated by equation 1, for the different clays are 96 % for montmorillonite samples, 80 % for laponite samples and finally 73 % for kaolinite composites. The evolution of the phase content for the different clays can be explained by the expanding effect observed in the two first clays that is not observed in kaolinite. The interparticle

aggregates observed on laponite also difficult, on the other hand, its exfoliation and is responsible for the lower γ-phase content when compared with the montmorillonite. As on the case of montmorillonite, the melting of these nanocomposite samples at temperatures above 200ºC, prevents the crystallization of the γ -phase. Fig. 8 (b) shows the transmittance of the different samples, which also increases for these clays with respect to pure PVDF. The highest transmittance is obtained for the nanocomposite with laponite, followed by montmorillonite and kaolinite. These results can be related to the different degree of crystallinity of the polymer within the nanocomposites, i.e., the higher the degree of crystallinity of the nanocomposites, the higher is the transmittance. This fact is confirmed by the degree of crystallinity obtained by DSC: laponite, the clay giving origin to the most transparent nanocomposite, is also the one with the highest degree of crystallinity (59%), followed by montmorillonite (51%) and kaolinite (46%).

The different interaction between the clays and the polymer matrix, leading to the different electroactive phase content and transparency is also supported by the dynamical mechanical measurements performed for the three types of nanocomposites with 0.5% of clay. The results are represented in Figure 9. The higher elastic modulus is observed for nanocomposites when prepared with montmorillonite and laponite, but a lower elastic modulus than PVDF is observed when the kaolinite is present. This fact can be explained by the larger expanding effect observed on montmorillonite and laponite, that allows larger interaction areas between the polymer and the layers of the clays and prevents the nanocomposite deformation. On the other hand, the kaolinite is not an expanding clay so, the contact area between this clay and the polymer is smaller, representing therefore a defect that acts as a rupture zone and facilitates the deformation.

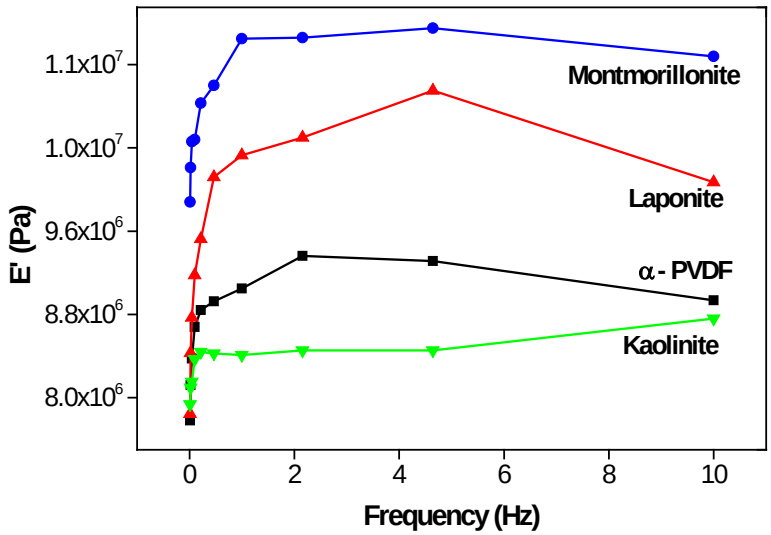

Figure 9. E' variation with frequency for α-PVDF and PVDF/clay nanocomposite with 0.50 % of montmorillonite, laponite and kaolinite.

Acknowledgements

This work is funded by FEDER funds through the "Programa Operacional Factores de Competitividade – COMPETE" and by national funds by FCT- Fundação para a Ciência e a Tecnologia, project references NANO/NMed-SD/0156/2007, PTDC/CTM/69316/2006 and PTDC/CTM-NAN/112574/2009. ACL also thanks the FCT for the grant SFRH/BD/62507/2009. The authors also thank support from the COST Action MP1003, the 'European Scientific Network for Artificial Muscles' (ESNAM).

References

(1) Gao, F., Mater Today, 2004, 7, 50-55.

(2) Pavlidou, S.; Papaspyrides, C.D., Prog Polym Sci, 2008, 33, 1119-1198.

(3) Schmidt, D.; Shah, D.; Giannelis, E.P., Curr Opin Solid St M, 2002, 6, 205-212

(4) Ueberschlag, P., Sensor Ver, 2001, 21, 118-125.

(5) Lovinger, A.J. Development in Crystaline Polymers; Basset, D.C, Ed.; Elsevier:London, 1982

(6) Sencadas, V.; Gregório Filho, R.; Lanceros-Mendez, S., J Non-Cryst Solids, 2006, 352, 2226-2229.

(7) Sencadas, V.; Gregório, R.; Lanceros-Mendez, S., J Macromol Sci B, 2009, 48, 514-525

(8) Martins, P.; Costa, C.M.; Appl Phys A-Mater, 2011, 103, 233-237.

(9) Mago, G; Fisher, F.T.; Kalyon, D.M; J Nanosci Nanotechno , 2009, 9, 3330-3340.

(10) Gregório, R; J Appl Polym Sci, 2006, 100, 3272-3279

(11) YuMing, S.; ZhuDi, Z.; WenXue, Y.; Bo, L.; 2007, 50, 790-796.

(12) Patro, T.U.; Mhalgi, M.V.; Khakhar, D.V.; Misra, A., Polymer, 2008, 49, 3486-3499

(13) Buckley, J.; Cebe, P.; Cherdack, D.; Crawford, J.; Ince, B.S.; Jenkins, M.; Pan, J.; Reveley, M.; Washington, N.; Wolchover, N., 2006, Polymer, 47, 2411-2422.

(14) Ince-Gunduz, B.S.; Alpern, R.; Amare, D.; Crawford, J.; Dolan, B.; Jones, S.; Kobylarz, R.; Reveley, M.; Cebe, P., 2010, Polymer, 51, 1485-1493.

(15) Ramasundaram, S.; Yoon, S.; Kim, K.J.; Park, C., J Polym Sci Pol Phys, 2008, 46, 2173-2187.

(16) Priya, L.; Jog, J.P., J Polym Sci Pol Phys, 2002, 40, 1682-1689.

(17) Priya, L.; Jog, J.P., J Polym Sci Pol Phys, 2003, 41, 31-38.

(18) Priya, L.; Jog, J.P., J Appl Polym Sci, 2003, 89, 2036-2040.

(19) Lanceros-Mendez, S.; Mano, J.S.; Costa, A.M.; Schmidt, V.H; J Macromol Sci B, 2001, 40, 517-527.

(20) Benz, M; Euler, W.B.;J Appl Polym Sci, 2003, 89, 1093-1100.

(21) Kressler, J; Schafer, R; Thomann, R.; Appl Spactros, 1998, 52, 1269-1273

(22) Bachmann, M.A.; Gordon, W.L.; J Appl Phy, 1979, 50, 6106-6112

(23) Silva, M.P.; Sencadas, V.; Botelho, G.; Machado, A.V.; Rolo, A.G.; Rocha, J.G.; Lanceros-Mendez, S.; Mater Chem Phys, 2010, 122, 87-92.

(24) Pinnavaia, T.J.; Butrulle, J.R., Characterization of Catalytic Materials, I.E. Wachs, I.E.; Fitzpatrick, L.E., Ed.; Butterworth-Heinemann: Boston, 1992, p. 149.

(25) Yao, Y.Z.; Kawi, S.; J Porous Mat, 1999, 6, 77-85.

(26) A. Salimi, A.A. Yousefi, Polymer test, 2003, 22, 699.

(27) Gregório, R.; Cestari, M., J Polym Sci Pol Phys, 1994, 32, 859.

(28) Miranda, D.; Sencadas, V.; Sánchez-Iglesias, A.; Pastoriza-Santos, I.; Liz-Marzán, L.M.; Gómez Ribelles, J.L.; Lanceros-Mendez, S., J Nanosci Nanotechno, 2009, 9, 2910.

(29) Xu, R.J.; Manias, E.; Snyder, A.J.; Runt, J., Macromolecules, 34, 337-339.

(30) Costa,C.M.; Gomes, J.; Serreno Nunes, J.; Sencadas, V.; Lanceros-Mendez, S., Int J Mater Prod Tec, 2010, 32, 178-185

(31) Zhu,X.; Zhu, J.; Zhou, S.; Li, Q.; Liu, Z.; Ming, N.; Meng, Z.; Chan, H.L.; Choy, C.L., Ferroelectrics, 2001, 263, 1367-1376

(32) Gomes, J.;Serrano Nunes, J.; Sencadas, V.; Lanceros-Mendez, S., Smart Mater Struct, 2010, 19, 065010

(33) Branciforti, M.C.; Sencadas, V.; Lanceros-Mendez, S.; Gregório, R., J Polym Sci Pol Phys, 2007, 45, 2793-2801.

(34) Leach, E.S.H.; Hopkinson, A.; Franklin,K.; van Duijneveldt, J.S., Langmuir, 21, 3821-3830.